Development of a Spin-Light Polarimeter for the EIC

April 20, 2012

Dipangkar Dutta (PI), James Dunne, Edward Leggett, Prajwal Mohanmurthy, Mitra Shabestari
Mississippi State University, Mississippi State, MS
Wouter Deconinck (Co-PI), Valerie Gray
College of William and Mary, Williamsburg, VA
Abhay Deshpande (Co-PI)
Stony Brook University, Stony Brook, NY
Frank Maas (Co-PI)
Johannes Gutenberg-Universität, Mainz, Germany
Kent Paschke (co-PI)
University of Virginia, Charlottesville, VA
Paul Reimer (Co-PI)
Argonne National Lab, Argonne, IL
Dave Gaskell (Co-PI)
Thomas Jefferson National Accelerator Facility, Newport News, VA

1 Abstract

We propose to develop a spin-light polarimeter to measure the electron beam polarization at the EIC. The proposed polarimeter requires a position sensitive hard X-ray detector. We will develop a pair of split-plane differential ionization chambers as position sensitive X-ray detectors. These will be tested using the chicane magnets of the Compton polarimeters at JLab. We also expect to reuse existing wiggler magnets from Argonne National Lab to build a prototype 3-pole wiggler magnet. The wiggler magnet together with the differential ionization chambers will be used to build a complete prototype spin-light polarimeter.

2 Introduction

Polarized electrons and ion beams are an essential part of the EIC program to address fundamental questions in QCD, such as how gluons contribute to the spin structure of the nucleon. The EIC also has a unique ability to measure parity-violating structure functions involving $W^{\pm}$ and Z boson mediated interactions. The EIC will enable precision tests of the Bjorken sum rule, a fundamental test of QCD, and thereby allow precision measurements of the strong coupling constant, α_s. It would also allow measurements of generalized parton distributions (GPD) and transverse momentum distributions (TMD), which would lead to 3-D mapping of the proton's internal structure. The high energy and luminosity combined with polarized electrons and protons as well as a variety of heavy ion targets will provide a wealth of data in a regime never explored before.

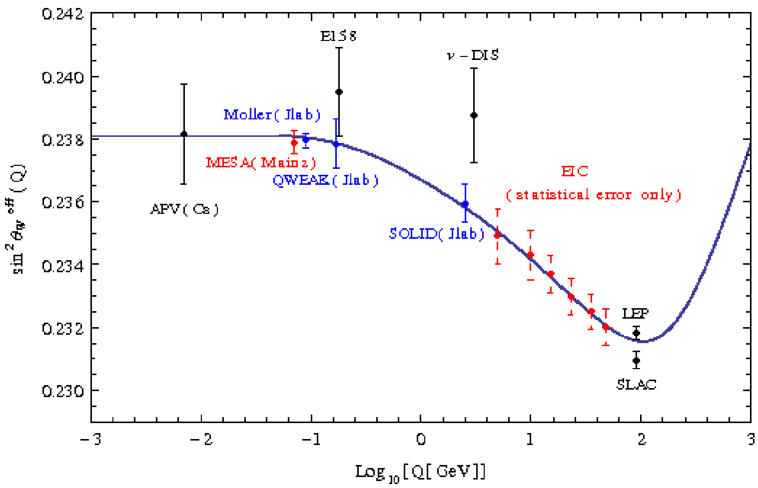

Figure 1: The projected uncertainties of past, present and future EIC measurements of $\sin^2\theta_W$.[1]

The parity-violating, right-left, deep-inelastic polarized *ep* and *ed* asymmetries can be used to precisely determine the running of $\sin^2\theta_W(Q)$ as a function of Q^2. The comparison of those measurements with precision values obtained from other lower energy or Z-pole studies can be used to find hints of "new physics". Alternatively, the overall world average of $\sin^2\theta_W$ can be compared with precisely determined quantities such as α_{EM}, G_F, m_Z, and m_W to test the SM at the quantum loop level and probe "new physics" effects. The projected uncertainties of past, present and future EIC measurements of $\sin^2\theta_W$ are shown in Figure 1 [1][1].

This entire program, especially the parity-violating electroweak program at the EIC, will place stringent requirements on the precision polarimetry of the electrons. The determination of the polarization of the electron beam is one of the dominant systematic uncertainties for this program. In order to achieve the desired high precision, the polarization of the electron beam must be monitored continuously with a systematic uncertainty of <1%. In addition to being precise, the polarimeters must be non-invasive and must achieve the desired statistical precision in the shortest time possible. These ambitious goals can only be achieved if multiple independent and high precision polarimeters are used simultaneously. We propose to develop a novel continuous non-invasive polarimeter based on the spin dependence of synchrotron radiation (SR), referred to as "spin-light". The proposed spin-light polarimeter can achieve 1% statistical precision in measurement cycles of less than few minutes. The proposed polarimeter would facilitate cross-checks and systematic studies, and the redundancy, both in the measurement and monitoring of the beam polarization, will provide a new benchmark in precision electron beam polarimetry. We present a description and a conceptual design of a spin-light polarimeter, and propose a R&D program to develop the detector technology which is essential for the success of a spin-light polarimeter.

3 A Spin-Light Polarimeter

The exact expression for SR intensity including quantum corrections was calculated by Sokolov, Ternov and Klepikov, based on the solution to the Dirac equation in the framework of quantum electrodynamics [2]. Sokolov and Ternov also developed the mathematics required to describe the spin of relativistic electrons moving in an external electromagnetic field [3, 4], which allowed them

[1]We thank Yingchuan Li for an updated version of this figure.

to calculate the electron spin related properties of SR. The spin dependence of the SR was verified at the VEPP-4 storage ring in Novosibirsk [5] for 5 GeV transversely polarized electrons. A related spin dependence known as the Sokolov-Ternov self polarization was first observed at the French storage ring [6] at Orsay and is now used to polarize beams at some circular electron accelerators.

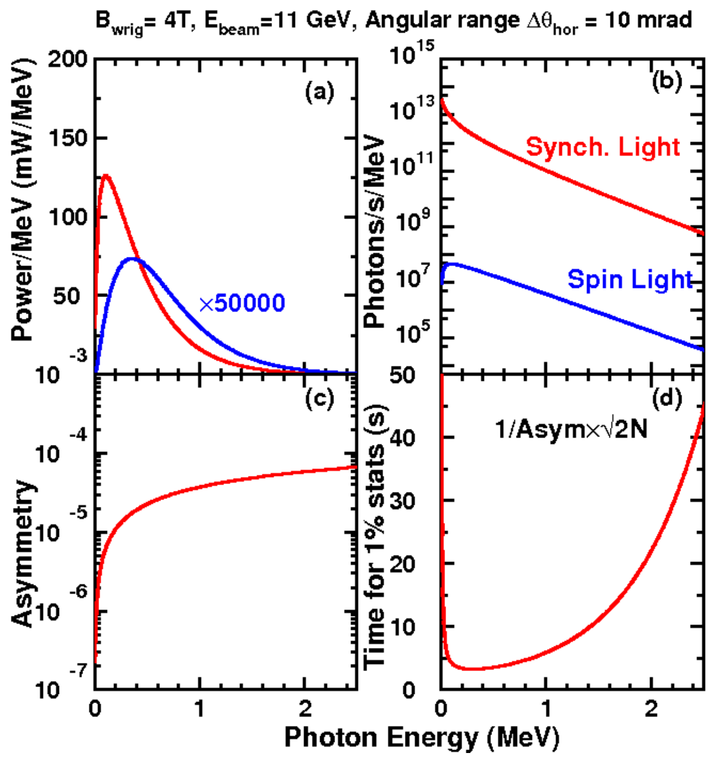

Figure 2: (a) The total SR power radiated, per MeV (red), and the spin dependent difference in power radiated, per MeV (blue), above and below the orbital plane, for 11 GeV, longitudinally polarized electrons in a 4 T magnetic field and 100 mA current, 1% collimation and 10% detector efficiency. (b) The total number of SR photons per MeV and the number of “spin-light” photons per MeV, and (c) the asymmetry $\frac{\Delta N}{N}$ as a function of photon energy. (d) The time for 1% statistical uncertainty, in seconds.

Ordinarily one would expect the quantum effects to become important if the acceleration of the electron is comparable to the acceleration at which a single SR photon would carry away all of the electron’s energy (called the critical condition). The critical magnetic field strong enough to provide this acceleration is found to be $B_c = \frac{m_e^2 c^3}{e\hbar} \sim 4{\times}10^9$ T and the critical energy $E_c = m_e c^2 \sqrt{\frac{m_e c R}{\hbar}} \sim 10^6$ GeV [3, 7], where e, m_e, and R are the charge, mass and orbital radius of the electron. Since the critical energy and field are extremely large compared to those accessible at present day terrestrial accelerators, the quantum corrections to the SR intensity in a magnetic field B and a Lorentz boost of γ, can be expanded in terms of the critical parameter $\xi = \frac{3}{2}\frac{B}{B_c}\gamma << 1$, and are therefore relatively small. However, it turns out that several quantum effects, such as the spin dependence of SR are important even at considerably lower electron energies and fields.

The total SR power, $S_\gamma(long)$, radiated by longitudinally polarized electrons is a function of n_e, the number of electrons, j, the electron spin polarization, ψ, the vertical angle in the frame of the moving electron and the ratio $y = \frac{\omega}{\omega_C}$, of the angular frequency of the SR photon (ω) and the critical angular frequency (ω_C). Ignoring spin flip terms and other terms of order ξ^2, the radiated power can be written in terms of the modified Bessel functions, $K_n(z)$, as [3]:

$$\begin{aligned} S_\gamma(long) &= S_\gamma + \Delta S_\gamma \cdot j \\ &= \frac{9n_e}{16\pi^3}\frac{ce^2}{R^2}\gamma^5 \int_0^\infty \frac{y^2 dy}{(1+\xi y)^4} \oint d\Omega (1+\alpha^2)^2 \times \\ & \left[K_{2/3}^2(z) + \frac{\alpha^2}{1+\alpha^2} K_{1/3}^2(z) + j \cdot \xi y \frac{\alpha}{\sqrt{1+\alpha^2}} K_{1/3}(z) K_{2/3}(z) \right], \end{aligned} \tag{1}$$

where $z = \frac{\omega}{2\omega_C}(1+\alpha^2)^{3/2}$, and $\alpha = \gamma\psi$ with ψ being the vertical angle. The spin dependent term in Eq. 1 is an odd function of the vertical angle therefore when integrated over all angle the total SR power for longitudinally polarized electrons is spin independent. However, the power radiated into the space above $(0 < \psi < \pi/2)$ and below $(-\pi/2 < \psi < 0)$ the orbital plane of the electron are different and the difference between them is spin dependent [3, 4]. This offers a new possibility for direct observation of the polarization characteristics of an electron beam by determining the difference in the SR power above and below the electron beam direction.

To examine the size and characteristics of this spin dependence we have numerically integrated Eq. 1 for $I_e = 100$ mA, $E_e = 11$ GeV, longitudinally polarized electron with 100% polarization, in a 4 Tesla magnetic field, with collimators that accept 1% of the total power and detection efficiency of 10%. We have integrated over a horizontal angular acceptance of $\Delta\theta = 10$ mrad, and a vertical acceptance of $\alpha = \pm 1$ rad. We show the results only at $E_e = 11$ GeV, but the entire EIC range of energies, E_e = 4 - 20 GeV, is accessible (see Fig 3(a)). The total power radiated by longitudinally polarized electrons, S_γ(long,) per MeV and the spin dependent difference in power radiated above and below the orbital plane of the electron (spin-light), ΔS, per MeV are shown in Fig 2(a). The number of SR photons, N_γ(long), per MeV and the number of spin-light photons ΔN_γ(long), per MeV, as function of photon energy are shown in Fig 2(b).

The asymmetry defined as $A = \frac{\Delta N_\gamma(long)}{N_\gamma(long)}$ as a function of photon energy is shown in Fig. 2(c). This indicates that one should measure the hard tail of the SR spectrum ($E_\gamma >$ 500 keV) and avoid the soft part of the spectrum where the asymmetry is low and changes rapidly with energy. Although the asymmetry is small $\sim 10^{-4}$ the photon flux is high, even at the hard tail of the spectrum, allowing a rapid determination of the asymmetry, integrated over photon energies, with 1% statistical uncertainty ($\frac{\delta A}{A} = \frac{1}{A\sqrt{2N}}$) within a few tens of seconds (Fig. 2(d)). The energy dependence of the asymmetry for $E_e = 4 - 20$ GeV and the magnetic field dependence of the asymmetry for $B_{wrig} = 2 - 5$ T are shown in Fig 3(a) and Fig 3(b) respectively. These figures demonstrate that a spin-light based polarimetry is a very promising technique at intermediate energies and can be used to monitor the polarization of $4 - 20$ GeV electrons in very rapid measurement cycles, with high statistical precision.

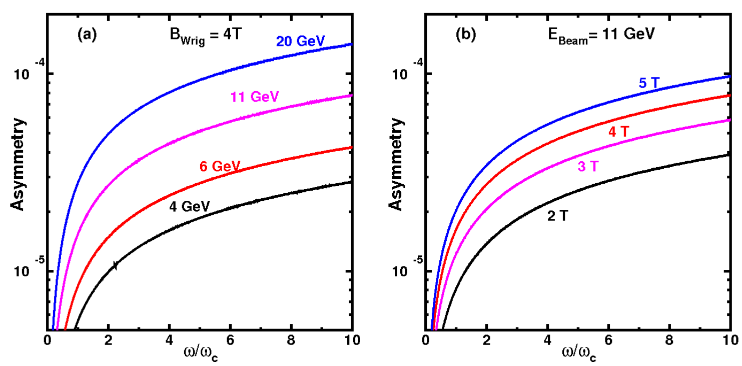

Figure 3: (a) The spin dependent asymmetry as a function of ratio of photon energy to the critical photon energy, for electron beam energy, $E_{beam} = 4 - 20$ GeV. (b) The spin dependent asymmetry for magnetic field, $B_{wrig} = 2 - 5$ Tesla.

3.1 A Conceptual Design

The two basic components of a spin-light based polarimeter are the source of SR and the X-ray detector which can measure the spatial asymmetry.

3.1.1 The SR Source - Wiggler

A three pole wiggler magnet with a magnetic field that has uniform magnitude but reversed direction at each pole and a short-long-short pole arrangement is well suited as a source of SR. The three poles must be symmetric about the center such that the line integral of the magnetic field in the direction of the motion of the electron, z, must be zero (i.e. $\int B(z)dz = 0$), ensuring that it does not effect the electron beam transport and its spin direction (beyond the wiggler). The magnitude of the field being constant at the 3 poles, flips the sign of the spin dependent spatial asymmetry from any two adjust poles and hence when measured simultaneously it can help reduce systematic uncertainties arising from the vertical motion of the beam.

The intensity and the asymmetry both increase with increasing field strength, while the pole length decreases with increasing field strength. Therefore a field strength of 4 T is a judicious choice for the wiggler field. A 10 mrad bend can be achieved with a pole length of 10 cm. Thus the total magnet length is 40 cm, and the spacing between the poles is optimized for ease of extraction and detection of the SR beam. A separation of 1 m between the poles allows for collimators to be placed that can separate the SR beams spots from the different poles. The small pole length ensures that the effect of spin-flip inducing SR and the fluctuation of the SR power are negligible ($< 0.1\%$).

The number of photons emitted by a particular electron per radian bend will be distributed according to Poisson statistics about a mean value given by [8], $n = \frac{5}{2\sqrt{3}}\frac{\gamma}{137} = 20.62E$, where n is the mean number of photons per radian bend, E is the beam energy in GeV. The average energy of the photons emitted is $E_c = \hbar\omega_c = \frac{3}{2}\frac{\hbar c\gamma^3}{R}$ [8]. Therefore the mean energy fluctuation is given by $\Delta E = \sqrt{n}E_c$. It is interesting to note that the energy fluctuation depends only on the electron beam energy and the bend radius of the wiggler. A beam of 11 GeV electrons in a 4T wiggler with a 10 m bend radius and a bend angle of 10 mrad, gives $n \sim 2$ and $E_c = 199$ keV. Therefore $\Delta E/E \sim 2.5\times10^{-5}$, which is comparable to the fluctuations due to the recirculating arcs of the JLab accelerator [9].

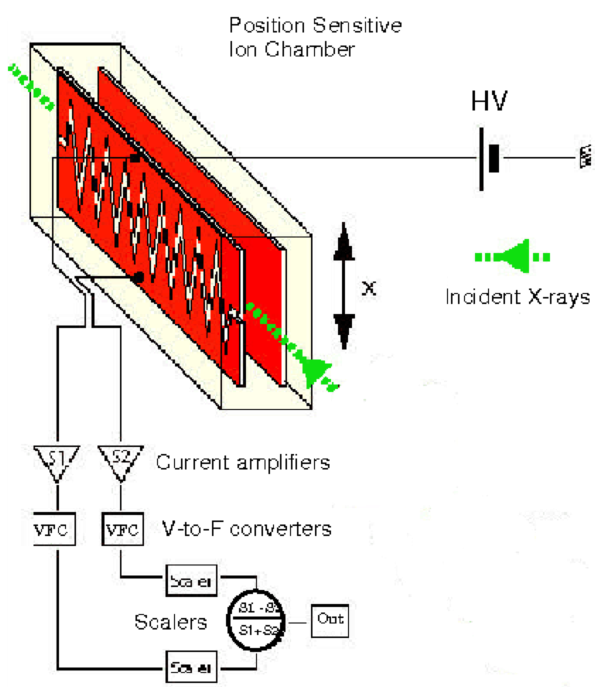

Figure 4: A position sensitive ionization chamber developed at the APS and SPring-8 with a resolution of 5μm when operated at photon flux of 5.0×10^{12} 8 keV photons/sec. [10]

The SR power spectrum usually peaks at angles of $\pm1/\gamma$ with respect to the electron direction. However, if an electron emits on the average two photons in a magnet, the angular distribution of the momentum kick received by each electron is peaked in the direction of the electron's motion. The magnitude of the transverse kicks generated by the emission of a photon with energy E_c in the direction $\theta_\gamma = 1/\gamma$ with respect to the electron direction is given by [8], $\Delta\theta_e = \frac{E_\gamma \sin\theta_\gamma}{E_e} = 11.3 \times 10^{-9} \frac{E_e(GeV)}{R(m)}$. The r.m.s. kick from the emission of n photons is given by $\sqrt{n}\Delta\theta_e$. Thus for a 11 GeV beam bend by 10 mrad the r.m.s. kick is $\sim 1.5 \times 10^{-8}$ rad, which is negligible.

Thus the wiggler magnet would have negligible influence on the electron beam and a spin-light polarimeter can be used for non-invasive monitoring of the relative beam polarization.

3.1.2 The X-ray Detector - Ionization Chamber

The detector used to measure the spatial asymmetry must be sensitive to ∼500 keV to 2.5 MeV X-rays and must be able to pick out a small asymmetry from a large spin independent background, it must be radiation hard, have low noise and be able to withstand high rates of $\sim 10^{12}$ photons/sec. Ionization chambers (IC) are well known for their high rate capability (when operated as an integrating detector (i.e. in current mode)), low electronic noise and radiation hardness. Argon/Xenon is an attractive candidate for use as an ionization medium, its high atomic number (18/54) and density (when compressed) gives it a high stopping power for hard X-rays and low energy gamma [11]. Another recent development, is the split collector ionization chamber that have turned the IC into a position sensitive device. Position sensitive ionization chambers are designed to have the collector plate split into two sections in a zig-zag/backgammon pattern such that each half operates as an independent ionization chamber. A prototype of such a chamber has been shown in Fig 4. These chambers were developed at the Advanced Photon Source at the Argonne National Lab and at the SPring-8 light source in Japan. They are used to measure the vertical position of X-ray beams and have been shown to have a resolution of 5 μm [10]. These chambers also have very low dark currents in the ∼pA range and have been operated at photon flux of 5.0×10^{12} photons/sec. They work by measuring the difference in counts between the two halves of the chamber, i.e. they are differential ionization chambers. A position sensitive differential ionization chamber operated in current mode can be used to measure the spatial asymmetry of the SR generated by longitudinally polarized electrons. A dual, 1 atm. Ar/Xe differential ionization chamber would be ideal for a relative polarimeter. A schematic for such an IC is shown in Fig. 5. The chamber would consist of Ti or stainless steel windows thick enough to cut down the low energy X-rays (< 50 keV). A split central collector/ground plate would be placed between the anode and the cathode. The collector plate would be split in a backgammon pattern. The current measured on each half of the collector plate is amplified with a current amplifier. The SR beam from two adjacent poles will be incident on the differential ionization chambers and the spin-light spatial asymmetry (above and below the orbital plane) will have opposite sign in the left/right halves of the DIC because the magnetic field direction of adjacent poles are opposite. On the other hand any spatial asymmetry due to vertical motion of the beam will have the same sign in the left/right halves of the DIC.

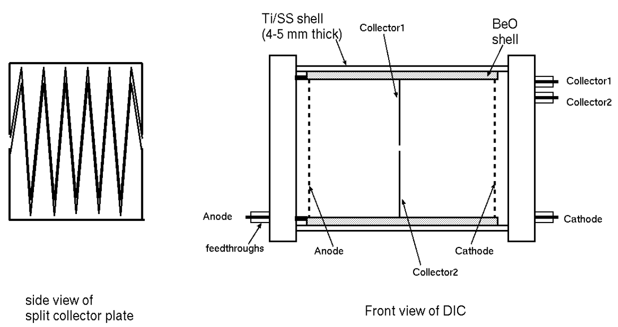

Figure 5: (left) A schematic of the split collector plate. (right) The differential ionization chambers.

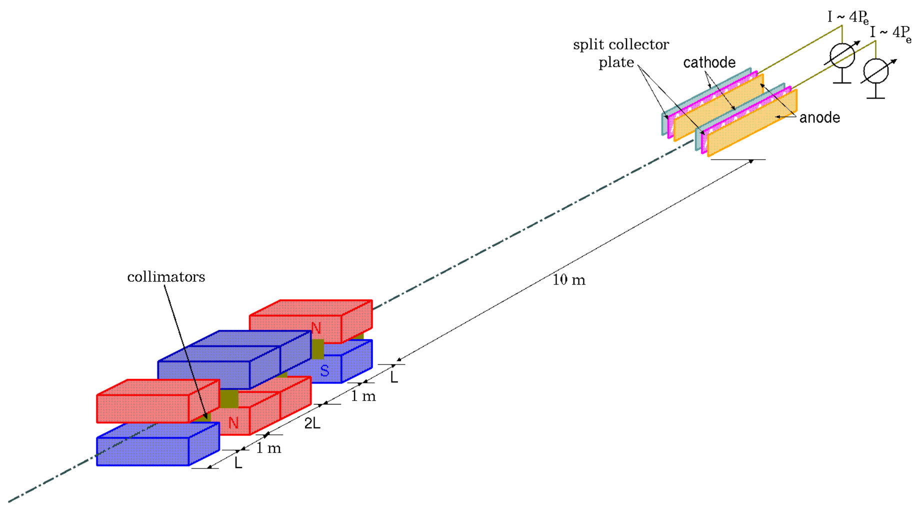

Figure 6: A schematic for a differential spin-light polarimeter (not to scale).

3.1.3 The Complete Polarimeter

A 3D view of the complete spin-light polarimeter is shown in Fig 6. It consists of the 3-pole wiggler magnet (the central pole is twice the length of the other two poles and will be treated as a combination of 2 identical poles for the rest of this proposal). Each pole of the wiggler magnet is separated by a distance of 1 m and the pair of differential ionization chambers are placed 10 m from the last pole of wiggler magnet.

The central backgammon plates of the two DICs are oriented with their splits along the vertical direction such that the DICs are position sensitive in the vertical direction. The magnet system will wriggle the beam by 10 mrad in the horizontal plane such that each pole of the wiggler magnet produces a fan of synchrotron radiation in the horizontal plane as shown in the top view of the magnets (Fig 7). For linearly polarized electrons this fan of synchrotron radiation will have an up-down asymmetry in the vertical direction (due to spin-light). A series of collimators placed at the front and back faces of each pole of the wiggler magnet and at the center of the central pole of the wiggler will be used to select small angular ranges from the entire fan of synchrotron radiation as shown in the top view of the magnets in Fig 8. This collimation scheme enables separation of the synchrotron

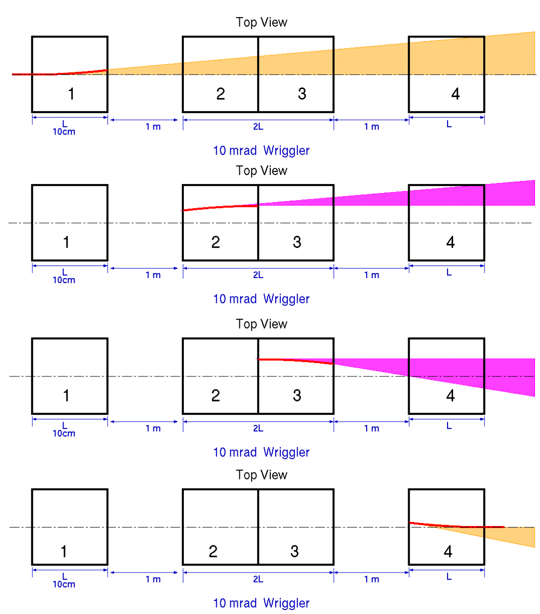

Figure 7: A schematic of the fan of synchrotron radiation produced as the electron beam traverses through each of the 4 poles of the wiggler magnet. The top view of the magnets is shown.

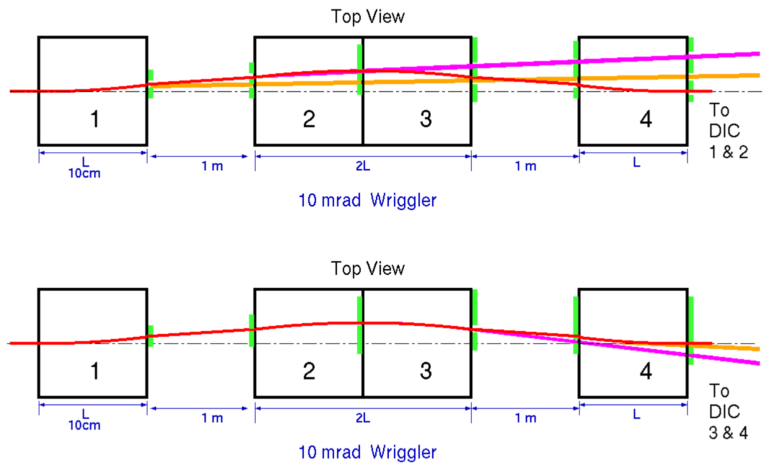

Figure 8: (left panel) A schematic for the slits and collimators used to select small angular range of the fan of synchrotron radiation. The synchrotron beams from poles 1 and 2 will be incident on the DIC placed on the beam left and the beams from poles 3 and 4 are incident on the DIC placed on the beam right.

radiation from each pole of the wiggler magnet. Such a separation is necessary because the up-down asymmetry of the synchrotron radiation has opposite sign for each pole of the wiggler. Each of the collimated beams of synchrotron radiation will be separated by a few cm when they are projected into the pair of differential ionization chambers located at a distance of 10 m from the wiggler magnet. A magnified view of the synchrotron radiation from two adjacent poles of the wiggler magnet incident on the left/right halves of one DIC is shown in Fig. 9. The left panel of the figure shows the beam's view of the DIC. The collimated radiation is shown as oval blobs with the up-down asymmetry represented by the gray shading of the blob. The right panel shows an isometric view of the electrodes in the DIC, without showing the incident radiation. The second pair of DIC (not shown in Fig. 9) is necessary to provide an independent measurement of the up-down asymmetry and help reduced systematic uncertainties. The vertical backgammon split on the central electrode makes the DIC position sensitive in the vertical direction and hence the signal from the DIC is sensitive to the up-down asymmetry for each of the 4 collimated beams of synchrotron radiation. The outer electrodes of each DIC has opposite polarity because the adjacent poles of the wiggler magnet reverse the sign of the up-down asymmetry.

3.1.4 The Signal from the DICs

If we denote $N_{SR}^{L(R)}$ as the number of SR photons on the left(right) of the collector plate, $N_{spin}^{L(R)}$ as the number of spin-light photons and $\Delta N_z^{L(R)}$ as the difference in number of photons introduce by the vertical beam motion, then the contribution to the measured current from the top left part of the DIC will be;

$$I_1^L \propto N_{SR}^L + N_{spin}^L + \Delta N_z^L,$$

similarly the current contribution from the top right of the DIC is;

$$I_1^R \propto N_{SR}^R - N_{spin}^R + \Delta N_z^R.$$

Note the change in the sign of the contribution from spin light photons because they are generated from adjacent poles of the wiggler while the contribution from vertical beam motion has the same

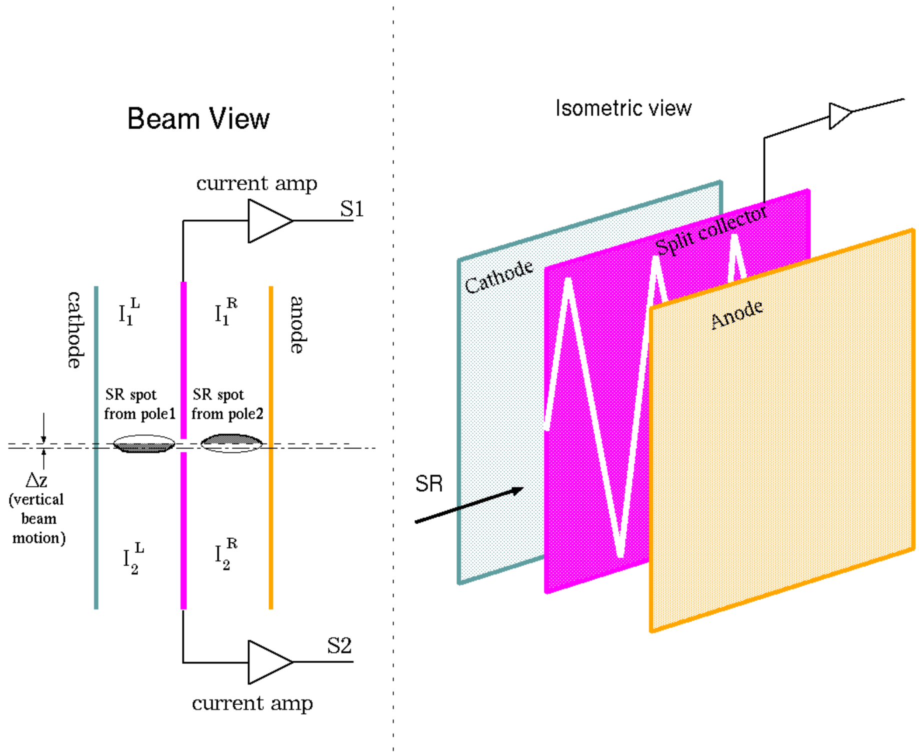

Figure 9: (right panel) A schematic of the collimated beams of synchrotron radiation from 2 adjoining poles of the wiggler magnet incident on the differential ionization chambers. The figure on the left is a beam's view of the electrodes of the DIC. The collimated radiation is shown as oval blobs, while the figure on the right is an isometric view of the electrodes.

sign. For the bottom left and right parts of the DIC we get;

$$I_2^L \propto N_{SR}^L - N_{spin}^L - \Delta N_z^L,$$

and

$$I_2^R \propto N_{SR}^R + N_{spin}^R - \Delta N_z^R.$$

Thus, the signal from the top and bottom halves of the DIC, $S1$, and $S2$ as shown in Fig. 5, can be written as,

$$S1 \propto (N_{SR}^L + N_{spin}^L + \Delta N_z^L) - (N_{SR}^R - N_{spin}^R + \Delta N_z^R) = 2N_{spin},$$

and

$$S2 \propto (N_{SR}^L - N_{spin}^L - \Delta N_z^L) - (N_{SR}^R + N_{spin}^R - \Delta N_z^R) = -2N_{spin}.$$

Hence $S1 - S2 \propto 4N_{spin} \propto 4P_e$, and the vertical motion related asymmetry cancels to first order. In addition it should be noted that the signals $S1 + S2$ is proportional to the transverse polarization of the electron beam. This possibility of measuring both the longitudinal and transverse asymmetries in the same setup, provides further capability for reducing systematic uncertainties and makes the spin-light polarimeter an extremely versatile tool.

The major sources of systematic uncertainties for a spin-light polarimeter are background asymmetries from processes such as Bremsstrahlung and false asymmetry due to vertical beam motion, differences in chamber efficiency and magnetic field non-uniformity between adjacent poles of the wiggler. The main advantage of operating the ionization chambers as differential detectors is that the false asymmetries will cancel to first order. In addition the visible portion of the synchrotron light can be used to align the detectors and help control systematic uncertainties. The 3-pole design ensures that the vertical beam motion related false asymmetry also cancels to first order. The background asymmetries can be monitored using the difference in the signal from the chambers with the wiggler magnets turned on and off. We estimate the systematic uncertainties of a relative polarimeter to be < 0.5 %.

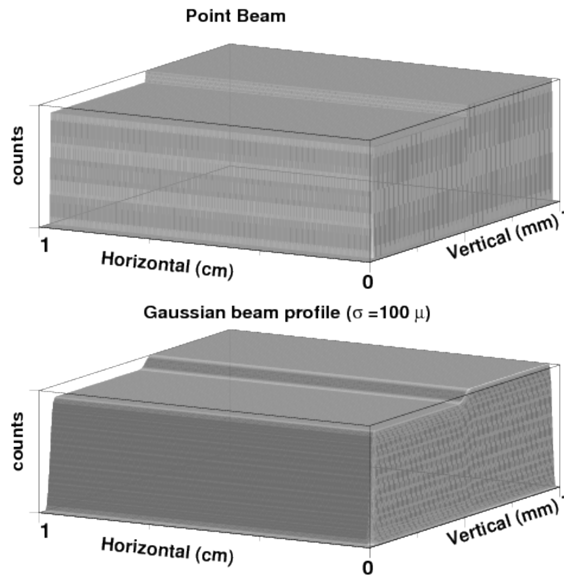

Figure 10: (upper panel) Simulation of the up-down asymmetry as seen by an ionization chamber for a point electron beam. A 1 cm$\times$ 1 mm rectangular section of the collimated SR beam is shown with the number of counts along the z-direction, the up-down asymmetry has been magnified to make it visible. (lower panel) Simulation of the up-down asymmetry as seen by an ionization chamber for an electron beam with a σ= 100 μm Gaussian distribution.

We have also simulated the effect of the finite beam size on the up-down asymmetry. Fig. 10 shows a rectangular section of the fan of synchrotron radiation incident on an ionization chamber. The section is 1 cm wide and has a height of 1 mm (the height of SR beam 10 m from the wiggler). The asymmetry between the synchrotron radiation above the orbital plane and below the orbital plane has been magnified to make it visible. The number of SR photons are shown along the axis rising out of the plane of the paper (z-direction). The upper panel shows the radiation for a point electron beam while the bottom panel shows the same for a beam with a Gaussian distribution of σ= 100 μm. This demonstrates that the up-down asymmetry due to the spin-light is not affected by the finite beam profile.

The effects of the fringe fields at the tapered edges of the wiggler poles has also been simulated using a Poisson Fish model of the magnetic field. Although the absolute photon flux was reduced due the fringe fields the effect on the asymmetry was founds to be minimal.

4 Plan of Work

Over the last five years the PI has setup a new detector lab at MSU (using startup funds) and has successfully built and characterized diamond multi-strip detectors, which were recently installed and used as electron detectors for the Hall-C Compton polarimeter during the QWeak experiment. This is the first diamond detector to be used at JLab. This project was funded by the U.S. Department of Energy (DOE). As part of the 12 GeV upgrade of Hall-C at JLab, the PI is building a gas electron multiplier (GEM) based active collimator for the SHMS spectrometer. This project is also funded by DOE. The PI has demonstrated the capability to adapt new emerging detector technology and built complex detectors.

We propose to construct a split plane differential ionization chamber as a prototype of the X-ray detector to be used in a spin-light polarimeter. The prototype differential ionization chamber will be tested using the existing chicane magnets of the Hall-A Compton polarimeter and a 11 GeV longitudinally polarized electron beam to measure the spatial asymmetry in SR from longitudinally polarized electrons. Such a measurement would be the first demonstration of the spin dependence of SR from longitudinally polarized electrons.

In parallel the William and Mary group will develop the complete simulations and the CCD based optical alignment system which will use the visible portion of the synchrotron radiation to help align the detector and monitor helicity correlated beam motion.

The ANL group has extensive experience with complex detector systems and large installation experiments. They can also help procure surplus wiggler magnets from the Advanced Photon Source at ANL.

The UVa group has extensive experience with the JLab Hall-A Compton polarimeter and their expertise will be invaluable during the testing of the differential ionization chambers in the Hall-A Compton beamline.

The Stony Brook and Mainz groups, both have extensive polarimetry experience at BNL and MAMI respectively.

The eRHIC design team at BNL, led by Dr. Vladimir Litvinenko and the EIC Task Force at BNL as well as members of the Center for Advanced Studies of Accelerators (CASA) at JLab will be consulted throughout this project and will aid in the design process.

The JLab group had extensive experience with the Hall-C Moller and Compton polarimeters and their expertise will be invaluable during the testing of the differential ionization chambers in the Hall-A Compton beamline.

4.1 Projected Time-line

4.1.1 Year 1

The PI and post-doc Mitra Shabestari from the MSU group will work on the simulation, design and construction of the split-plane differential ionization chamber. Graduate student Valerie Gray from the William and Mary group will also work on this project. The Mainz group has extensive polarimetry experience and will provide engineering assistance during the design phase of the project.

1. Simulation and Design
A Geant simulation of the split-plane ionization chamber will be developed. The geometry of the split-plane will be studied in these simulations to help select the best geometry to maximize the position resolution and stability. This work will be performed by the W&M group and the UVa group.

A Geant simulation of the Synchrotron radiation and spin-light radiation will be carried out using field maps of the Hall-A Compton chicane magnets. This will help determine the expected signal and ideal location for the detector. This work will be performed by the W&M group and the UVa group.

2. Hardware
Ionization chambers and power supplies will be procured. Current amplifiers and other readout electronics will be procured and tested. This will be carried out by the MSU.
A DAQ system will be setup to test the ionization chamber using radiological sources. This work will be performed by the MSU group.

3. Deliverables
Final design of the split-plane geometry.
Optimized running conditions and detector location.
Tested DAQ setup.

4.1.2 Year 2

The design, construction and demonstration of the differential ionization chamber will be completed in the first two years of the project.
1. Simulation and Design
A Geant simulation of the dual split-plane ionization chamber for the full proto type polarimeter. Verify optimized split plane for dual chamber.
Design and implement prototype wiggler magnet in the Geant simulation of the Synchrotron radiation and spin-light radiation. This will help optimize the wiggler design and determine the ideal location for the detector. The same simulation will also help in the design of the CCD system for the detection of the visible portion of the synchrotron radiation. This work will be performed at W&M and the UVa group. Engineering assistance with the design of the split-plane chamber will be provided by the University of Mainz

2. Hardware
Build the split-plane for the ion chamber based on results of simulation from year 1.
Assemble split plane ion chamber along with all readout electronics and DAQ developed during year 1. Perform tests of the split-plane ion chamber in the lab using radiological sources. These tasks will be performed at MSU.

3. Deliverables
A well tested split-plane ion chamber ready for testing in the Hall-A Compton chicane magnets.

4.1.3 Year 3

The testing of the prototype chamber in the Hall-A Compton beamline will be completed over the second and third period. Co-PI Dr. Kent Paschke and his group had worked on both the Hall-A and Hall-C Compton polarimeters and they will help carry out the testing of the differential ionization chambers in the Hall-A Compton beamline. During the third years the complete set of prototype differential ionization chambers (four) will be constructed in the detector lab at MSU. The PI and post-doc will design the chambers based on the tests of the prototype detector, to be carried out in the Hall-A Compton beamline. Design and engineering assistance will be provide by University of Mainz group. During this period the full time effort of a post-doc may be needed.

During this period, we will begin the process of identifying an existing 4 Tesla prototype wiggler magnets for the spin-light polarimeter. One of the co-PIs Dr. Paul Reimer (Argonne National Lab), will help identify such a wiggler magnet. Wiggler magnets are routinely built at light sources such as the Advanced Photon Source (APS) at ANL and Spring8 in Japan. Some of these magnets are well suited for a spin-light polarimeter. [12]. We expect to begin the process of identifying, procuring and adapting an appropriate wiggler magnets from the APS.

The beamline vacuum elements and collimators for the spin-light polarimeter will be constructed in consultation with the members of Center for Advanced Studies of Accelerators (CASA) at JLab. Dr. Arne Freyberger and Dr. Jay Benesch from CASA will collaborate on the design of the beam line elements of the spin-light polarimeter. Engineering assistance will be provide by University of Mainz group.

The W&M group will put together the CCD based alignment and beam motion monitoring system during this period.

Once the complete prototype is built an appropriate accelerator site, such as the storage ring in Novosibirsk, will be identified to help test the prototype. Co-PIs, Dr. Abhay Deshpande will help in identifying a suitable test site and organize the effort to test the prototype polarimeter.

1. Simulation and Design
Complete simulation and design of a full prototype polarimeter with dual ion chamber, and final design of wiggler magnet. The simulations will also help design the collimators needed and help determine the optical location of the collimators.

2. Hardware
Test the prototype split-plane chamber developed over year 1 and 2 with the JLab Hall-A Compton chicane magnets.
Identify a wiggler magnet for prototype polarimeter based on simulations of year 2.
Procure dual ionization chamber based on simulations of year 2.
Assemble dual chamber with optimized split-planes, read out electronics and DAQ.
Build beamline vacuum elements for prototype polarimeter including slits and collimators.
Build CCD alignment and beam motion monitoring system.

3. Deliverables
A prototype split-plane ionization chamber tested with polarized electron beam.
All detector and vacuum systems for a prototype spin-light polarimeter that is ready to be tested in an appropriate electron beam facility.

Summary

5 Budget

5.1 Salaries

Funds are requested to support half a post-doc at MSU for all three years. Funds are also requested for half a graduate student at William and Mary for all 3 years. Matching funds are available for the post-doc salary and the graduate student salary. Fringe and overhead is included for both post-doc and graduate student salaries. The post-doc salary is set at $42,000 and the graduate student stipend is set at $20,000 per annum.

Activity	Year 1	Year 2	Year 3
Design and build prototype DIC	$\surd$	$\surd$	
Test DIC in Hall A Compton beamline			$\surd$
Design CCD based alignment system	$\surd$	$\surd$	
Design and build set of dual DIC			$\surd$
Build CCD system			$\surd$
Design wiggler magnet		$\surd$	
Design slits and collimators		$\surd$	
Identify suitable wiggler magnet at the APS			$\surd$
Select suitable site to test prototype polarimeter			$\surd$

5.2 Equipment

During the first two periods a prototype split plane ionization chamber will be built. These will be based on commercially available chambers with a custom made collector plate. The chambers will be long and thin, 30 cm long with an electrode gap of 2.0 cm. The cost of the ion chambers is based on quotes from FMB Oxford. These chambers would then be modified by incorporating a custom electrode with a backgammon split. Several different periods and overlap lengths will be tried. The cost for the split electrodes is based on communication with I. Kuzmenko of the CMS-CAT at the APS. The price for the electronics to read out the ion chambers is based on quotes from FMB-Oxford. The price for power supplies are based on quotes for several different power supplies such as Iseg and Ortec.

The gas handling system for the ion chambers will be very similar to the system built for the GEM detector by the BoNuS collaboration at JLab. The P.I. is part of the collaboration and the price for the gas handing system is based on the P.I.s involvement in the building of the BoNuS detector.

Following the testing of the prototype DIC is the Hall-A Compton beamline, the dual split electrode DICs will be built for the polarimeter. These will have to be custom chambers adapted form the FMB-Oxford chambers. The price for these chambers is based on the price for similar size chambers from FMB-Oxford.

The associated readout electronics for the dual chambers include current amplifiers, V-to-F converters and scalers. They also include additional power supplies for the dual chambers. The price for these are based on quotes from FMB-Oxford, Iseg and Ortec

The price for the custom beamline vacuum elements which will help mount the detectors is based on quotes from MDC vacuum. They also include slits and collimators. The price for the slits and collimators are based on quotes from FMB-Oxford who specialize in building slits and other detector mounting elements for synchrotron light sources.

The CCD based alignment system will consist of a remotely controllable multi-axis motion stage, associated motor controllers and driver. The price for these items is based on several quotes from motion stage manufacturers such as Dover Motion and IKO. The cost of CCD system, readout and DAQ is based on similar systems being used at the Duke FEL Lab and quotes from Thorlabs.

Equipment	Total cost
prototype DIC	10000
Split plane electrodes	5000
Electronics for DIC(2 channels)	
current amps	8000
High voltage power supplies	10000
V-to-Fs and scalers	15000
VME crate	10000
Single board computer	7000
Gas Handling system	10000
The Dual DICs	
Custom dual DICs	12000
with split collector	
additional amps	8000
Custom beamline vacuum	10000
elements	
slits and collimators	8000
CCD alignment system	
motion stage, controller and driver (2)	16000
CCD imager and fast readout (2)	9000
light transport optics (2)	5000
Total Equipment Cost	143000

Table 1: Equipment cost breakup

5.3 Travel

Funds are requested in each of the three years of the grant to cover domestic travel related to traveling to collaboration meetings and travel to JLab during the later years for testing of ion chambers in the beamline. Travel expenses include overhead charges.

5.4 Total

The year by year breakdown of the budget along with the total request of $344000, is shown in table 5.4.

Item	Year 1	Year 2	Year 3	Total
0.5 Post-doc (MSU)	$40k	$40k	$40k	$120k
0.5 Grad student (W&M)	$17k	$17k	$ 17k	$51k
Equipment	$46k	$49k	$48k	$143k
Travel	$10k	$10k	$10k	$30k
Total	$113k	$116k	$115k	$344k

References

[1] D. Boer *et al.*, arxiv:1108.1713

[2] A. A. Sokolov, N. P. Klepikov and I. M. Ternov, JETF **23**, 632 (1952).

[3] A. A. Sokolov and I. .M. Ternov, *Synchrotron Radiation*, Pergamon Press, New York (1968); A. A. Sokolov and I. .M. Ternov, *Radiation from Relativistic Electrons*, A.I.P. Translation Series, New York (1986).

[4] I. M. Ternov, Physics - Uspekhi **38**, 409 (1995).

[5] S. A. Belomesthnykh *et al.*, Nucl. Inst. and Meth. **227**, 173 (1984).

[6] J. Le Duff, P. C. Marin, J. L. Manson, and M. Sommev, Orsay - Rapport Technique, 4-73 (1973).

[7] I. M. Ternov, Nucl. Instr. and Meth., 152, 213 (1978).

[8] M. Sands, SLAC Technical note, SLAC-121 (1970).

[9] B. Norum, CEBAF Technical note, TN-0019 (1985).

[10] K. Sato, J. of Synchrotron Rad., **8**, 378 (2001); T. Gog, D. M. Casa and I. Kuzmenko, CMC-CAT technical report.

[11] A. E. Bolotnikov and B. Ramsey, Nucl. Inst. and Meth. **A396**, 360 (1997).

[12] E. Nakamura *et al.*, J. of Elec. Spec. and Rel. Phen. **80**, 421 (1996); D. E. Baynham, P. T. M. Clee, and D. J. Thompson, Nucl. Instr. and Meth., **152**, 31 (1978)